Nonlinear numerical modelling and experimental validation of multilayer piezoelectric vibration energy scavengers

D. Blažević *[a], S. Zelenika [a]

[a] University of Rijeka, Faculty of Engineering & Centre for Micro and Nano Sciences and Technologies, Vukovarska 58, 51000 Rijeka, CROATIA

ABSTRACT

Scavenging of low-level ambient vibrations i.e. the conversion of kinetic into electric energy, is proven as effective means of powering low consumption electronic devices such as wireless sensor nodes. Cantilever based scavengers are characterised by several advantages and thus thoroughly investigated; analytical models based on a distributed parameter approach, Euler-Bernoulli beam theory and eigenvalue analysis have thus been developed and experimentally verified. Finite element models (FEM) have also been proposed employing different modelling approaches and commercial software packages with coupled analysis capabilities. An approach of using a FEM analysis of a piezoelectric cantilever bimorph under harmonic excitation is used in this work. Modal, harmonic and linear and nonlinear transient analyses are performed. Different complex dynamic effects are observed and compared to the results obtained by using a distributed parameter model. The influence of two types of finite elements and three mesh densities is also investigated. A complex bimorph cantilever, based on commercially available Midé Technology® Volture energy scavengers, is then considered. These scavengers are characterised by an intricate multilayer structure not investigated so far in literature. An experimental set-up is developed to evaluate the behaviour of the considered class of devices. The results of the modal and the harmonic FEM analyses of the behaviour of the multilayer scavengers are verified experimentally for three different tip masses and 12 different electrical load values. A satisfying agreement between numerical and experimental results is achieved.

Keywords: piezoelectric energy scavenging, vibrations, FEM, experimental assessment, multilayer cantilever

1. INTRODUCTION

The process of harvesting low-level environmental energy and its transformation into electric energy used to power low consumption devices such as ubiquitous wireless nodes, designated as energy scavenging, is widely studied and applied, especially when coupled to microsystems technologies, wearable devices or the internet-of-things. Photovoltaic, thermoelectric, triboelectric, electromagnetic or RF energy scavenging principles are thus being investigated and applied in wireless technology but also healthcare, transportation, communication systems, structural health monitoring, robotics, MEMS and many other potential application sectors. Scavenging of kinetic oscillatory energy via the bending of metallic cantilevers coated with thin piezoelectric films (Fig. 1) is particularly advantageous in this regard, especially in surroundings where photovoltaic or thermoelectric scavenging is ineffective due to the absence of direct sunlight or inadequate thermal gradients. The piezoelectric vibration scavenging concept is also characterised by design simplicity, miniaturization and integration potential, high energy densities per device volume and the linearity of the mechanical behaviour and of the coupling of mechanical and electrical domains. In fact, the selection of the dimensions of the cantilever and of the tip mass allows the tuning of the first bending eigenfrequency of the scavenger, usually the most prominent and used one, to the harmonic excitation of its base, characterised by its period and amplitude [1-7].

A suitable mathematical model of the coupled electromechanical behaviour of piezoelectric vibration energy scavenging devices with distributed parameters has recently been proposed [8]. Although the model, based on the classical Euler-Bernoulli beam assumptions, allows taking into account the backward coupling of the piezoelectric effect on the mechanical response, it is computationally rather complex and easily applicable only to simpler cantilever design configurations and load conditions. To assess the performances of piezoelectric vibration scavengers, in many instances a finite element analysis modelling approach is hence still preferred [9-13]. In fact, finite element models (FEM) allow the coupled-field analysis, needed to simulate the overall behaviour of the considered class of devices, to be effectively applied, while being adaptable to different geometric and other boundary conditions.

* dablazev@riteh.hr; phone + 385 – (0)51 – 651585; fax +385 – (0)51 – 651416; www.riteh.uniri.hr & www.cmnzt.uniri.hr

Smart Sensors, Actuators, and MEMS VII; and Cyber Physical Systems, edited by José L. Sánchez-Rojas, Riccardo Brama, Proc. of SPIE Vol. 9517, 95171F · © 2015 SPIE
CCC code: 0277-786X/15/$18 · doi: 10.1117/12.2178138

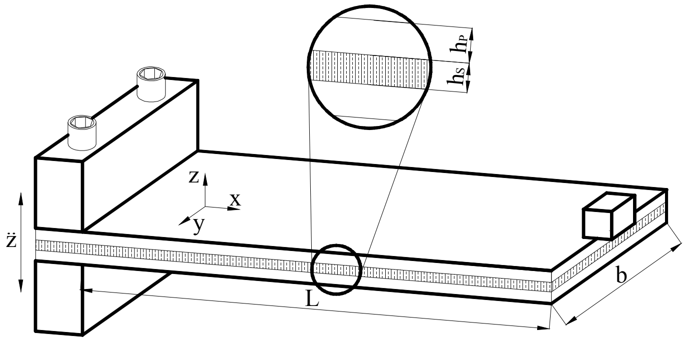

Figure 1. A piezoelectric energy scavenging bimorph with a tip mass: h_s indicates the substrate thickness, h_p the piezoelectric layers' thicknesses.

A conventional approach of using a FEM analysis of a simple piezoelectric cantilever bimorph under harmonic base excitation is thus used in section 2 of this work. Several analyses are performed on the same model: modal, harmonic as well as linear and nonlinear transient analysis. Different dynamic effects are hence observed and then compared to the results obtained by using the mentioned distributed parameter model implemented in MATLAB®. A comparison of the influence of two types of finite elements and three mesh densities is also investigated.

In the third section of the paper, a complex bimorph cantilever, based on commercially available Midé Technology® Volture series of energy scavengers, is considered. These scavengers are characterised by an intricate multilayer structure not investigated so far in literature. In fact, instead of the three layers found in conventional piezoelectric bimorphs (Fig. 1), these devices consist of nine layers.

An experimental set-up is developed in section 4 to evaluate the behaviour of the considered class of devices. The results of the modal and the harmonic FEM analyses of the behaviour of the multilayer scavengers are verified experimentally in the fifth section of the paper for three different tip mass values and 12 different electrical resistance values. A satisfying agreement between the numerical and the experimental results is achieved, especially regarding the prediction of the maximal obtainable powers up to a commonly used level of electrical loads.

2. NUMERICAL MODELLING OF BIMORPH VIBRATION ENERGY SCAVENGERS VIA THE FEM APPROACH

The ANSYS® FEM software package [14-15] has been proven to be an effective tool for predicting maximum electrical powers obtainable from piezoelectric scavenging systems, while a combination of SPICE® and ANSYS® software packages has been proposed for accurate prediction of the complex coupled dynamics of the herein investigated systems [9-11]. To verify the coupled-field analysis capabilities of the employed ANSYS® software, a conventional approach of using a 3D finite element model of a bimorph piezoelectric cantilever under harmonic base excitation is employed first in this work (Fig. 2). Several analyses are performed on the developed model: modal, harmonic, transient linear and nonlinear. Different dynamic effects are thus observed and compared to the results obtained by using the experimentally verified coupled modal electromechanical distributed parameter model implemented in MATLAB® [1, 16-17]. A comparison of the influence of different types of finite elements and mesh densities is also investigated.

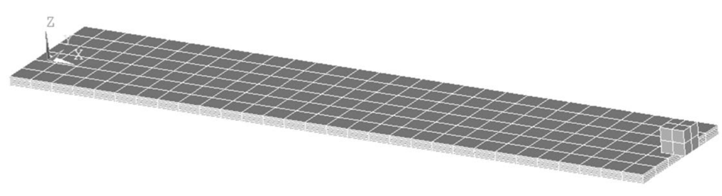

Figure 2. 3D ANSYS® finite element model of a three-layer piezoelectric energy scavenging bimorph with a tip mass.

2.1 Modelling procedure

A simple bimorph cantilever is employed as a 3D ANSYS® study model (Fig. 2). The cantilever consists of two outer piezoelectric layers made from PZT-5A ceramics [18], an inner substrate steel layer and a tungsten tip mass. The usually applied epoxy bonding layers are disregarded, and the three structural layers are considered perfectly bonded to each other and to the tip mass. Ultra-thin electrodes, which cover the surface of the piezoelectric material, are also disregarded. The dimensions and material properties used in the model are accordingly reported in Table 1.

Table 1. Dimensional and material properties of the modelled piezoelectric bimorph cantilever.

Piezoelectric bimorph feature	Symbol	Unit	Value
Cantilever length	L	mm	100
Cantilever width	b	mm	20
Substrate height	h_{s}	mm	0.5
Piezoelectric height	h_{p}	mm	0.4
Substrate Young's modulus	E_{s}	N/m^2	$20.6 \cdot 10^{10}$
Piezoelectric Young's modulus	$\bar{c}_{11}^{E}$	N/m^2	$61 \cdot 10^{9}$
Substrate density	ρ_s	kg/m^3	7850
Piezoelectric density	ρ_{p}	kg/m^3	7800
Tip mass density	ρ_{M_t}	kg/m^3	19250
Tip mass weight	M_{t}	g	1
Piezoelectricity coefficient	$\bar{e}_{31}$	C/m^2	-10.4
Permittivity constant	$\varepsilon_{r\,33}^{S}$	-	830
Cantilever mechanical damping (estimated)	ζ	-	0.008
Cantilever capacitance (calculated)	C_{p}	nF	76.6

Prior to modelling the cantilever structure by employing the ANSYS® parametric design language (APDL), suitable finite element types have to be selected [14]. Two appropriate element types are included in the ANSYS® element database for the piezoelectric layers: SOLID226 3D brick elements with 20 nodes and 5 degrees of freedom per node and SOLID227 3D tetrahedral elements with 10 nodes and 5 degrees of freedom per node. Complementary substrate and tip mass elements are chosen so as to match the element shape and available node quantity of the piezoelectric elements: SOLID186 3D brick elements with 20 nodes and 3 degrees of freedom per node and SOLID187 3D tetrahedral elements with 10 nodes and 3 degrees of freedom per node. On the other hand, for simulating the electrical circuit elements, ANSYS® offers a distinct type of elements named CIRCU94, that are thus used in the considered coupled analysis for mimicking the electrical load (i.e. electrical resistances).

Modelling of the bimorph piezoelectric cantilever starts then by defining the selected elements and their material properties. The prismatic model volumes are defined next, separately for the piezoelectric layers, the substrate layer and the tip mass. At this point, volumes with matching material properties and chosen finite element types are attributed and meshed with a defined mesh density. As the volumes are still separate entities, they need to be bound together at the respective interfaces via node merging. To comply with the assumptions of the coupled electromechanical modal model used as reference, the tip mass is modelled here so that its centre coincides longitudinally with the free edge of the cantilever. On the other hand, the boundary conditions related to the clamped end of the cantilever are achieved by immobilizing all degrees of freedom of all end nodes of the clamped end.

In order to ensure the extraction of electrical charge from the piezoelectric layers, and having disregarded in the model the actually used thin electrodes, the nodes with electrical degrees of freedom on the piezoelectric layer surfaces are all linked to a conforming main node that serves as a connecting point for the formation of the electric circuit. Four main extraction ("drain") nodes, simulating the electrodes on the surfaces of the piezoelectric material, are selected and all the corresponding surface nodes are connected through them. This approach simulates perfectly conductive electrodes and in this regard matches the assumption of the coupled electromechanical analytical model used as reference. Since in a first instance only the mechanical dynamic behaviour of the bimorph is considered, the extraction nodes are not yet connected to each other or to the electric circuit to be formed by the CIRCU94 electric resistance elements.

Related to the bimorph's width, height and thickness, three diverse mesh densities, marked respectively with G1, G2 and G3 (each with a double increase in mesh density with respect to the previous one – Fig. 3), are then used to perform a mesh sensitivity analysis against the results obtained by using the mentioned coupled modal electromechanical distributed parameter model [1].

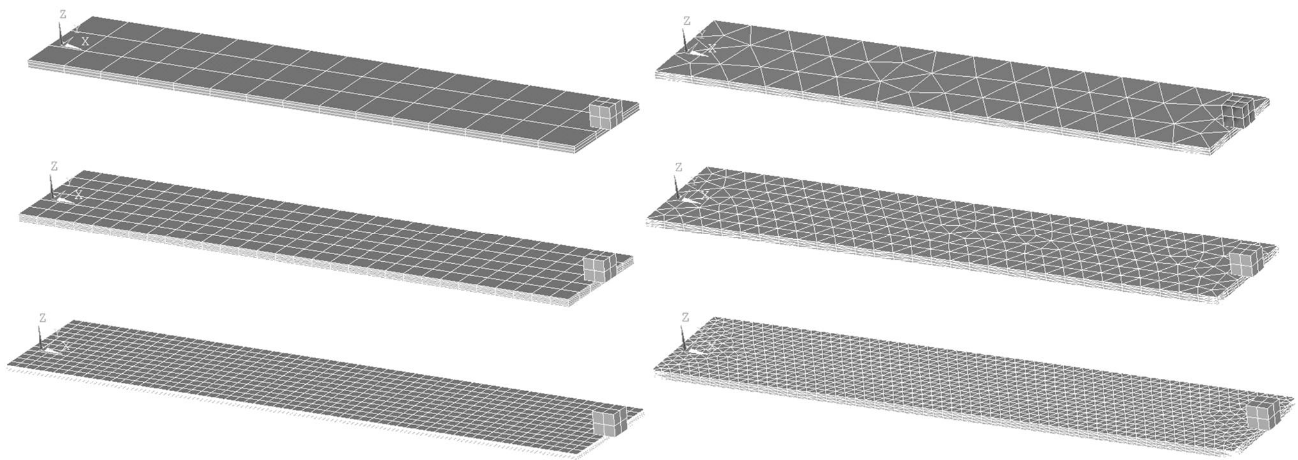

(a) (b)

Figure 3. User defined mesh densities G1, G2 and G3 (top to bottom): brick elements (a) and tetrahedral elements (b).

2.2 Modal analysis

Modal analysis is performed first in order to assess the mechanical dynamic response of the bimorph cantilever as well as to verify the coupling of all the merged layers and the validity of the imposed boundary conditions (Fig. 4). To this end, the values of the first bending eigenfrequency, i.e. the one commonly used in the energy scavenging process, obtained by using the described FEM model, are compared with those calculated in MATLAB® via the coupled modal electromechanical distributed parameter analytical model. For the FEM analyses, a sparse direct solver is chosen as the most robust solution that, however, is also the most intensive concerning computer memory usage. The comparison is performed by taking into account the two element types and the three mesh densities of Fig. 3.

Regardless of the considered mesh density and element type, the eigenfrequencies resulting from the FEM modal analyses are in perfect agreement (relative errors < 1%) with the analytically obtained first bending eigenfrequency of 57.1 Hz. This implies that generally FEM modal analyses can be performed with a coarser mesh.

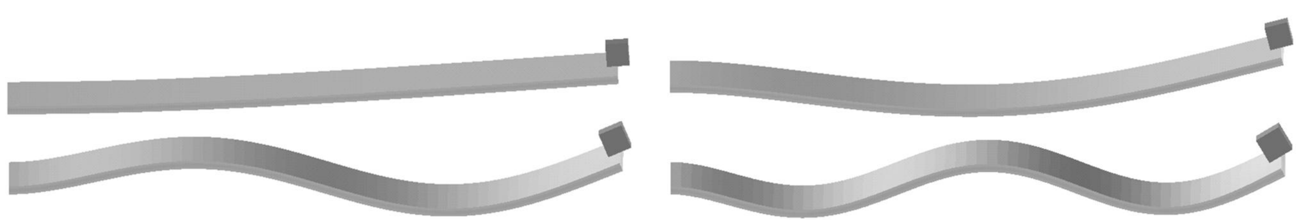

Figure 4. First four fundamental bending modes of the energy scavenger bimorph with a tip mass, with the first bending mode visible in the top left corner.

2.3 Harmonic analysis

Having assessed the proper mechanical dynamic response of the numeric model of the considered piezoelectric scavengers, the model can be coupled electromechanically by connecting the piezoelectric layers via the described main charge-collecting nodes into either a series or a parallel connection with the nodes of the CIRCU94 electric resistance elements. In the following FEM harmonic analyses and the corresponding coupled electromechanical analytical model, a series electrical connection is considered. In the FEM model the nodes of the CIRCU94 resistance elements are thus coupled on one side with the main charge extraction nodes at the surfaces of the piezoelectric layers interfacing the metallic substrate layer of the bimorph, and on the other side with the two charge-collecting nodes at the two outer piezoelectric surfaces. The harmonic analyses are then performed with suitable excitation amplitudes in a frequency range around (± 5 Hz) the first bending mode of the cantilever. The multiplication coefficients α and β of the mass and stiffness matrices, that are related to the considered frequency range and the effective damping [19], are determined based on previously conducted experiments [16] and set to, respectively, $\alpha = 2.9$ and $\beta = 2.04 \cdot 10^{-5}$. The steady state output voltages are monitored then on the nodes of the electrical resistance elements. A single resistive electrical load $R_l = 100$ kΩ is employed in both the FEM and the analytical calculations.

From the obtained results depicted in Fig. 5 it can be concluded that in the case of brick elements a higher mesh density does not bring about any improvement (Fig. 5a). In the case of tetrahedral elements, however, only the results obtained with the finest mesh (that designated with G_3) converge to those obtained with the brick elements (Fig. 5b). The maximal voltage outputs and respective eigenfrequencies of the FEM harmonic model clearly match very well (relative errors of, respectively, ≈ 2% and < 1%) with the values attained via the coupled electromechanical distributed parameter analytical model implemented in MATLAB®. This confirms the suitability of the FEM model in successfully predicting the electromechanical coupling and its influence in shifting the eigenfrequency from the previously calculated uncoupled value of 57.1 Hz to the newly determined value of 59 Hz. The observable differences in curve shapes can probably be attributed to previously determined ANSYS® limitations in performing energy scavenging simulations due, apparently, to the theoretical formulation of the direct piezoelectric effect adopted in the ANSYS® software package [11].

By performing equivalent harmonic analyses with increasing electrical load values (12 resistance values in the range from 10 Ω to 2 MΩ are considered here), the predicted backward coupling influence of the piezoelectric effect on the mechanical response of the bimorph [16-17], inducing a 2.5% rise of the respective eigenfrequencies (i.e. a hardening effect) can also be clearly seen (Fig. 6a). Comparing, however, directly, as shown in Fig. 6b, the output voltage levels and the eigenfrequencies obtained via the FEM and the analytical calculations, it can be seen that the FEM model induces an underestimate of the output voltage levels for electrical loads higher than ~ 100 kΩ (although still allowing a good prediction of the eigenfrequencies), which confirms the postulated limitations of the ANSYS® software [11].

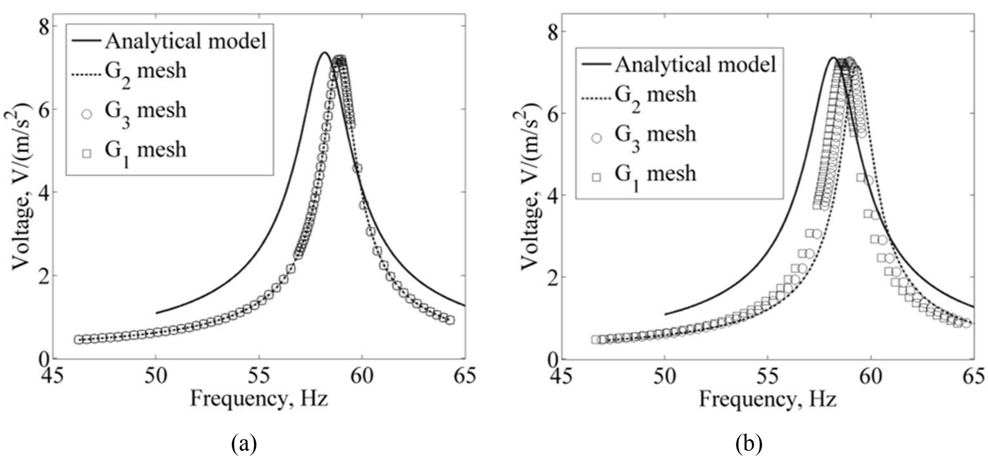

Figure 5. Comparison of output voltages normalized to excitation amplitudes obtained by using the FEM harmonic analyses (with brick (a) and tetrahedral elements (b) and different mesh densities) vs. the results of the coupled electromechanical distributed parameter analytical model.

2.4 Transient analysis: linear and nonlinear case study

The employed coupled electromechanical analytical model based on the Euler-Bernoulli beam theory (assuming, among others, that the cross sections of the cantilever remain plain during bending [20]), as well as the harmonic FEM simulations, are linear and do not take into account the nonlinear geometrical effects. Geometrical nonlinearities, or large deformation effects [21], occur when deformations become large enough to cause a twisting of the cross-sections of the cantilever (including also the anticlastic effect [22-23]). In the case of the herein considered energy scavenging cantilevers, these effects are to be expected if the devices are used next to their resonant state, i.e. when the largest amount of mechanical energy is to be converted to electrical energy. In this case, the stress-strain relationship might take a nonlinear form and the stiffness of the device might change, thus making the dynamic response of the device dependant on the excitation amplitude. If geometrical nonlinearities are to be considered within the FEM software, a transient analysis has to be used and the energy scavenging system under forced base excitation is hence modelled at discrete time steps in the frequency range of interest. A steady state response at each frequency increment allows then the respective voltage levels to be obtained. If the geometrical nonlinearity option is checked in the ANSYS® model by setting the NLGEOM option to ON [14], the software takes automatically into account for each time step the dependence of cantilever's stiffness on the newly reached node positions (i.e. on the deformations) and recalculates the respective stiffness matrix. The transient analysis option in ANSYS® does not, however, allow a direct definition of the excitation frequency or, alternatively, the definition of the acceleration amplitude for a desired frequency sweep. To overcome this restriction, the displacement profile of the clamped end of the scavenger with a tip mass was pre-programmed in MATLAB® by utilizing the following excitation profile definition: constant acceleration amplitude of 1 m/s^2, 16 data points per harmonic period and a frequency sweep range from 57.5 to 59 Hz with 0.05 Hz increments and 16 full cycles completed before the next step (to capture the steady state response). This excitation profile results in nearly 8000 data points (Fig. 7a) so that only short frequency intervals can be considered in reasonable simulation runtimes (10 h). The obtained profile is exported via a .csv file to an ANSYS® data table and the resulting Z displacements of cantilever's clamped end are iteratively changed through a DO loop (the motion of the clamped end nodes being still constrained in the X and Y directions). The resistive load is concurrently kept at 100 kΩ, while, due to a more favourable run speed-to-error ratio, the G_1 brick elements mesh configuration is employed.

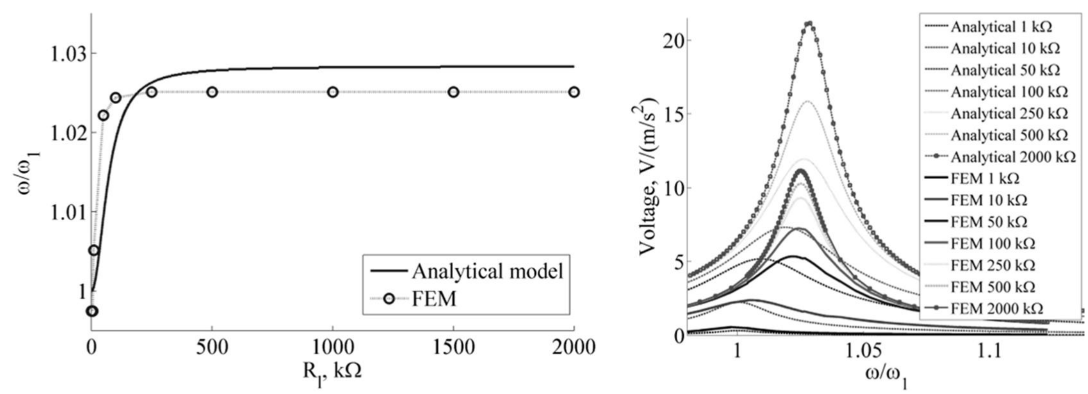

(a) (b)

Figure 6. Hardening effect obtained numerically and analytically for increasing electrical loads (10 Ω – 2 MΩ) (a) and direct comparison of analytically and numerically obtained voltages and eigenfrequencies for loads in the 1 kΩ – 2 MΩ range (b).

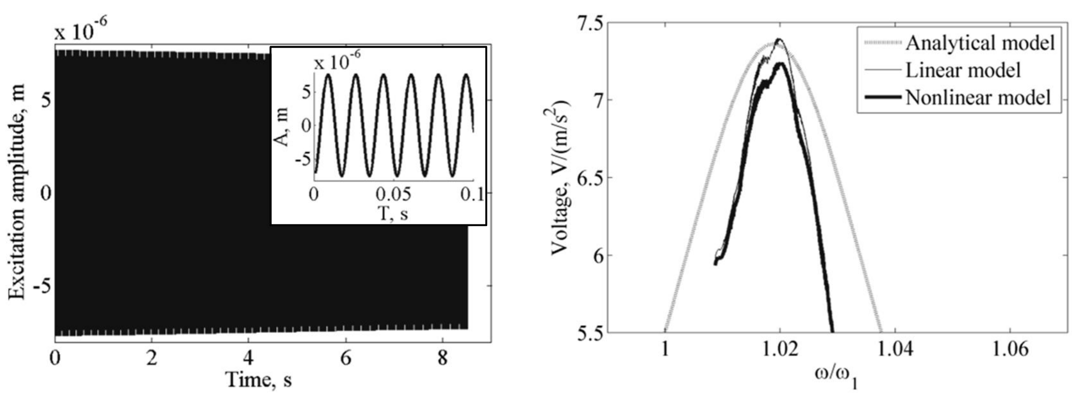

(a) (b)

Figure 7. Frequency dependent displacement profile of the clamped end of the scavenger (a) and comparison of transient analysis voltage outputs in a frequency range normalized to the uncoupled eigenfrequency (b).

The comparison of the results of the linear and nonlinear transient analysis runs, depicted in Fig. 7b, shows an excellent correlation with the implemented analytical model, especially concerning the obtained maximum voltage levels and the frequency shift induced by backward coupling. The error is now significantly lower than in the harmonic simulations and amounts to merely 0.05% when predicting the eigenfrequency with either linear or nonlinear transient analysis. The achieved maximum voltage levels are also in excellent agreement with the analytical model and display an error that is now around 1%. The maximum voltage levels obtained via the nonlinear analysis is ~ 2% lower than that obtained by using the linear transient analysis, showing that the effects of the geometrical nonlinearities are rather limited. Voltage curve shapes are still different from the ones obtained by employing the electromechanical analytical model; this can once more be probably attributed to the ANSYS® limitations concerning the simulations of energy scavenging systems.

3. FINITE ELEMENT MODEL OF MULTILAYER PIEZOELECTRIC VIBRATION ENERGY SCAVENGERS

Commercially available energy scavenging piezoelectric cantilevers present commonly a different structure than the bimorphs conventionally investigated in literature. In fact, the theoretically most investigated cantilever scavengers consist of only two piezoelectric layers and a single substrate layer while, as done above as well, epoxy glue and thin electrode layers are generally disregarded. Contrary to that, commercial scavengers of the considered type have usually additional protective layers that cover the piezoelectric materials' outer surface and serve as a shield against mechanical damage, whereas the width of the piezoelectric material itself may or may not extend to the edges of the substrate. For this reason, commercially available Midé Technology Corp.® Volture series scavengers, models V21B and V25B [24-25], are considered here for further numerical and experimental investigations.

3.1 Characteristics of Midé® Volture scavengers V21B and V25W

Midé® Volture scavengers (Fig. 8) are amongst the first cantilever devices designed specifically for scavenging low level environmental vibration energy by employing the direct piezoelectric effect. If compared to an ordinary piezoelectric bimorph, the structure of these devices is far more complex and consists of nine layers (Fig 9a) [24-25]: two outer protective FR4 sheets, four epoxy layers, two piezoelectric PZT-5A (CTS 3195HD) layers and a copper clad conductive polyimide Espanex® SB substrate layer. FR4 is a fire retardant outer layer made of woven fiberglass cloth with an epoxy resin binder on one side and a Cu electrode on the other that, given also its thickness (Table 2), significantly increases the stiffness of the device. On the other hand, the epoxy layers are very thin and are mostly squeezed out during manufacturing [24-25].

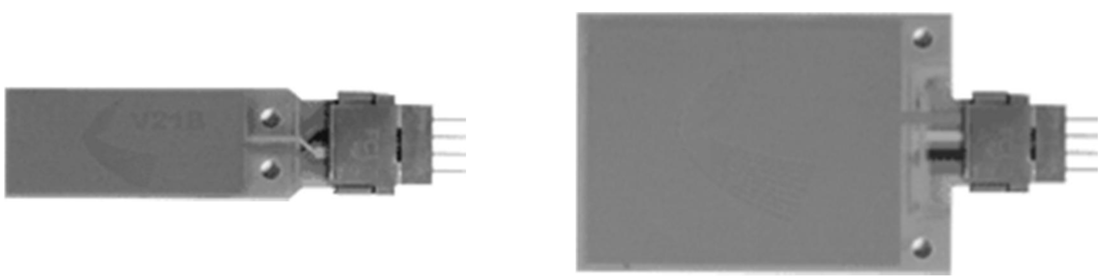

(a) (b)

Figure 8. Midé® Volture scavengers V21B (a) and V25W (a) [Midé Technology Corp.®].

3.2 Finite element model of the Midé® scavengers

In the above section 2 of this work, the approach for arranging a FEM numerical model for a conventional three-layer bimorph cantilever scavenger is described. The same methodology is applied here to model numerically the V21B and V25W geometrical configurations of multilayer Midé® Volture scavengers of Fig. 8. The models are based on the equivalent cross section shown in Fig. 9b (to allow greater control of the stiffness in the numerical model, the FR4 layer is broken up in the epoxy and the copper part), whereas the corresponding dimensions and material properties, derived from catalogues and available literature [24-28], are reported in Tables 2 and 3. The mechanical damping coefficient needed for the model is experimentally determined based on the customary logarithmic decrement technique. For each scavenger type, three standard Midé® tungsten tip masses (2.4, 4.8 & 7 grams for the V21B cantilever and 7.8, 15.6 & 23.4 grams for the V25W cantilever) are considered in the FEM analyses, resulting in six different numerical models.

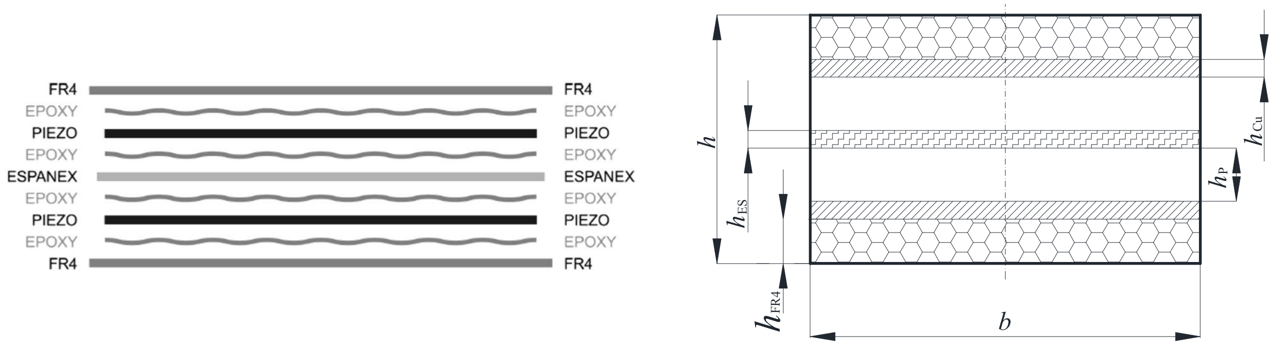

(a) (b)

Figure 9. Midé® Volture scavenges layers' composition (a) [Midé Technology Corp.®] and a CAD representation of the cross-section structure used for FEM analyses (b).

Table 2. Midé® Volture scavengers' dimensions and layer thicknesses.

Midé Volture scavenger dimension	Symbol	Unit	V21B	V25W
Free length	L	mm	33.8	46.25
Total width	b	mm	16.6	39.5
Piezoelectric layer thickness	h_p	μm	225	200
Espanex® layer thickness	h_{ES}	μm	25	25
FR4 layer thickness w/o copper electrodes	h_{FR4}	μm	120	100
Copper electrode layer thickness	h_{Cu}	μm	35	18

Table 3. Midé® Volture scavengers' material properties.

Material property	Symbol	Unit	Value
Young's modulus for copper	E_s	GPa	110
Young's modulus for PZT measured at a constant electric field	$E_p=\bar{c}_{11}^{E}$	GPa	67
Young's modulus for Espanex®	E_{ES}	GPa	4.5
Young's modulus for FR4	E_{FR}	GPa	23.4
Copper density	ρ_s	kg/m³	8940
PZT density	ρ_p	kg/m³	7800
Espanex® density	ρ_{ES}	kg/m³	1430
FR4 density	ρ_{FR}	kg/m³	1920
Tungsten density (tip mass)	ρ_{Mt}	kg/m³	19250
Piezoelectricity coefficient	$\bar{e}_{31}$	C/m²	-11.585
Permittivity constant measured at constant strain	$\varepsilon_{r\,33}^{S}$	-	830
Mechanical damping (experimentally determined)	ζ	-	0.006
V21B cantilever capacitance	C_p	nF	26
V25W cantilever capacitance	C_p	nF	130

Two main differences, related to the boundary conditions imposed by the experimental set-up, are introduced in the herein considered FEM models with respect to the modal and harmonic analyses described in section 2. In fact, in this case the tip mass position is placed with its outer edge coinciding longitudinally with the free end of the cantilever, whereas the clamped end is modelled according to the practical execution of the experimental clamp with two prismatic beams connected by nuts and bolts (cf. also Fig. 11). The latter condition implies that, contrary to the immobilization all degrees of freedom of all the nodes of the clamped end considered in section 2, here only the top and bottom nodes of the clamped end are fully constrained (Fig. 10a), while the degrees of freedom of the inner nodes of the respective cantilever cross section are not constrained. Given the above shown limited influence of the nonlinear effects as well as the computational intensiveness and continuance of the transient analyses, only modal and harmonic analyses are then performed. For the same reasons, a coarser mesh based on brick elements is chosen (Fig. 10b).

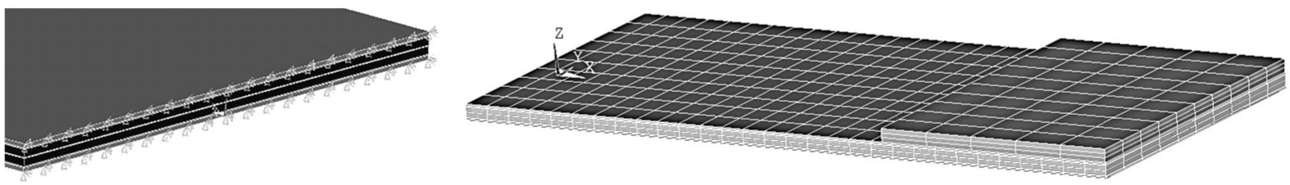

(a) (b)

Figure 10. Realistic clamped end boundary condition (a) and a meshed FEM representation of the whole Midé® Volture scavenger (b – shown is the model of the V21B scavenger with a 2.4g tungsten tip mass at the free end).

4. EXPERIMENTAL SET-UP

In order to validate the results obtained by performing the FEM modal and harmonic analyses of the commercially available multilayer piezoelectric vibration scavengers, an experimental set-up is put in place at the collaborating Laboratory of Mechanics of the University of Udine, Italy. The set-up, shown in Fig. 11, consists of a MB Dynamics PM25A shaker [29], a piezoelectric Bruel&Kjaer 4375 accelerometer [30], a suitably clamped Midé® Volture scavenger [24-25] and a Micro-Epsilon Messtechnik optoNCDT 1605 laser Doppler vibrometer [31] used for measuring the displacements of the free end of the cantilever. The laboratory shaker is driven via a Bruel&Kjaer 2635 signal amplifier [32], which in turn amplifies the waveform produced via the Bruel&Kjaer 1047 harmonic signal generator [33]. The set-up is interfaced to a National Instruments NI PXI-1042 controller [34]. Based on the readings from the accelerometer, this regulating unit is employed to alter the displacement amplitude of the shaker so as to keep the excitation acceleration amplitude at a constant level (0.633 m/s^2) throughout the experimental frequency sweeps (cf. in this regard also the description of the excitation profile of section 2.4). The NI system concurrently serves also to acquire the data from the laser vibrometer as well as the values of the output voltages from the energy scavengers.

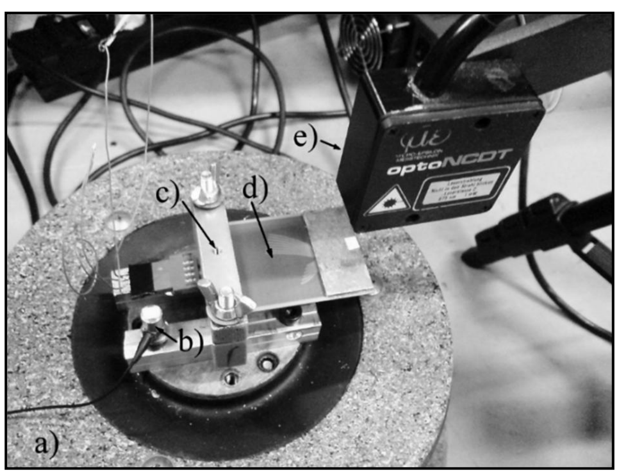

Figure 11. Experimental set-up: a) shaker, b) accelerometer, c) clamp, d) Midé® Volture scavenger, e) laser vibrometer.

In a first instance, quick impact tests are performed on the cantilever to identify its first bending eigenfrequency. A series of repetitive measurements is then conducted for each considered cantilever scavenger loaded with three different standard Midé® tungsten tip masses in a narrow frequency band (± 3 Hz) around its eigenfrequency. The tip masses are bonded to the cantilever by means of a low adhesion glue. Though assuring a proper junction and quick drying, the bonding allows for subsequent easy mounting and dismounting of the tip masses. Resistive loads are applied via simple potentiometers connected in series with the electrodes of scavengers' piezoelectric layers; R_l values used in the experiments are: 0, 21.9, 66, 111, 156.2, 206, 219, 262, 333, 421, 502, 606 and 651 kΩ. Although the potentiometers do not represent a realistic downstream load to be used in concrete applications, they allow for fast and simple change of the resistive load values in a broad domain, thus allowing for fast characterization of system's dynamics in numerous load conditions.

5. COMPARISON OF NUMERICAL AND EXPERIMENTAL RESULTS

The results obtained from the FEM analyses described in section 3 and the experimental results obtained by using the set-up detailed in section 4 are compared and validated in this part of the work. In this frame, the time dependent voltage values collected from the experiments are normalized with the excitation acceleration amplitude and transformed into the frequency domain via a fast Fourier transform. The experimental result sets are then plotted against the harmonic FEM numerical results for each cantilever scavenger type and corresponding tip mass weights, and for six different resistive loads chosen from the 12 values used in the experiments. Figure 12 shows a trend comparison of the resulting data sets for scavenger type V21B (Fig. 12a) and V25W (Fig. 12b). It can be noticed that the numerical model generally follows the dynamics behaviour of each experimental run thus indicating a proper coupling of the mechanical and electrical domains. Due to a large number of loads and narrow curves in Fig. 12, a more detailed comparison, performed separately for each tip mass, is necessary. Scavenger V21B results are chosen for the comparative study.

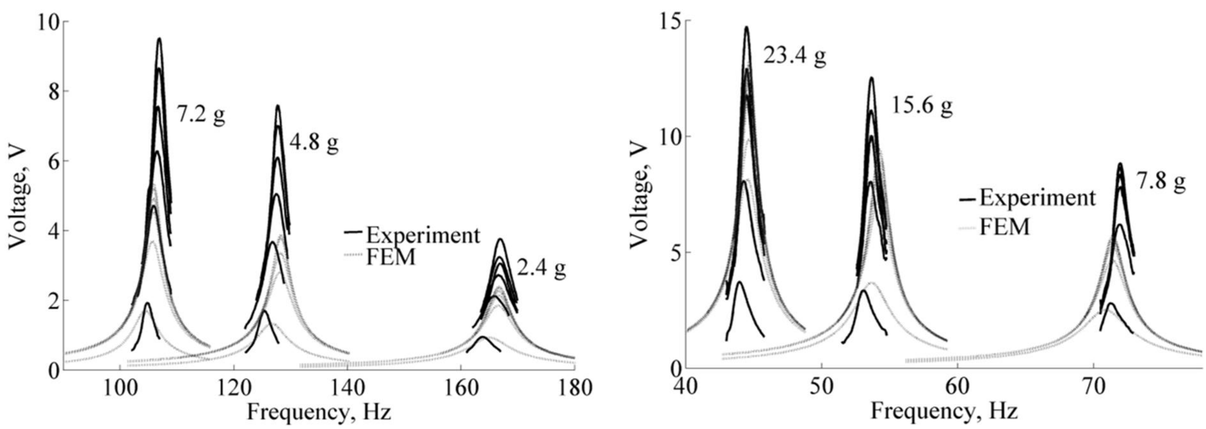

(a) (b)

Figure 12. Comparison of experimental and numerical results for six resistive load values (21.9, 111, 219, 333, 502 and 651 kΩ) and three tip masses for Midé® scavengers of type V21B (a) and V25W (b).

In Fig. 13 are hence visible in detail the differences emerging from the direct comparison of experimental and numerical results for the V21B Midé® scavenger for three tip masses and four resistive loads (21.9, 111, 333 and 651 kΩ). It can thus be seen that the numerical model adequately predicts the experimentally measured backward coupling hardening effect that causes the rise in the eigenfrequencies with increasing resistive loads. In fact, the discrepancy between the experimental and FEM eigenfrequency values is generally lower than 1% in all of the considered cases. On the other hand, however, the voltage level discrepancies are large and show an acceptable error of 2% only in the case of the lowest tip mass (2.4 g) and the lowest resistive load value (21,9 kΩ – Fig. 13a). In all the other cases, the errors on the values of the maximal output voltages is in average larger than 25%, with the discrepancies increasing for larger resistive loads, which once more substantiates the limitations of the ANSYS® software package in modelling energy scavenging systems.

The illustrated results can also be arranged so as to allow a better observation of the hardening of the cantilever scavenger structure occurring due to the backward piezoelectric coupling effect [1, 16]. In fact, by applying increasing resistive loads, a larger part of the vibration energy is converted into electrical energy and drawn from the system via the extraction of electric charge from the piezoelectric layers. This induces an asymptotic stiffening of the structure itself, which becomes clearly visible (Fig. 14) when the coupled eigenfrequency ω (influenced by the induced electric field) is normalized by the uncoupled (purely mechanical) eigenfrequency ω_1 and plotted against the resistive load values R_l.

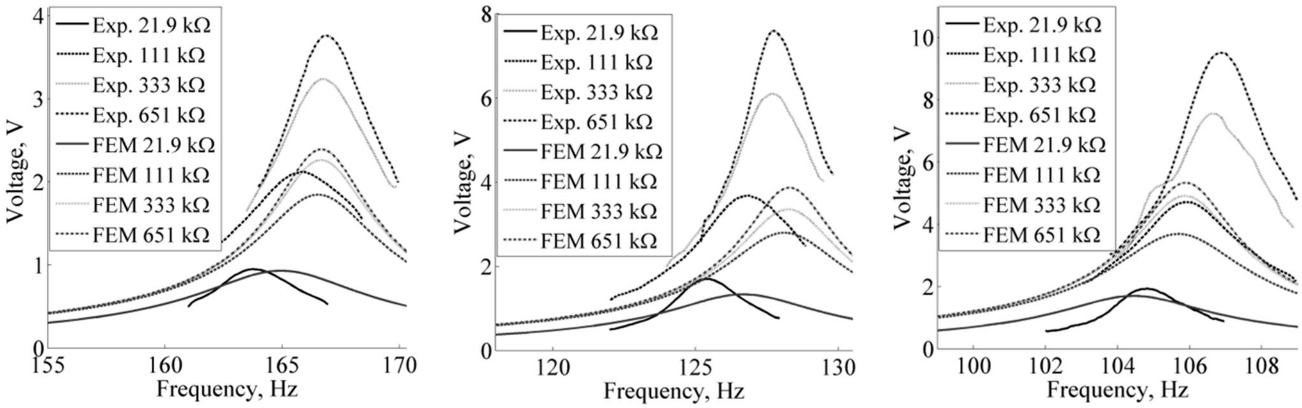

(a) (b) (c)

Figure 13. Comparison of experimental and numerical results for the Midé® V21B scavenger obtained with four resistive loads and three tip masses: 2.4g (a), 4.8g (b) and 7.2g (c).

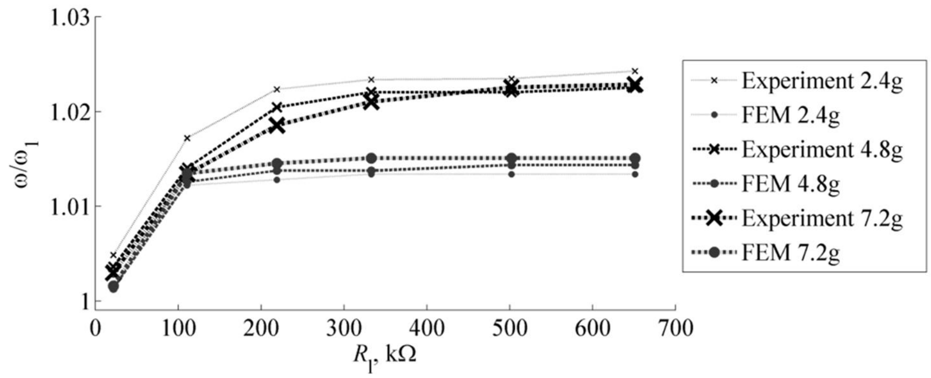

Figure 14. Comparison of FEM and experimental results of the electromechanical hardening effect for the Midé® V21B scavengers with three tip masses.

6. CONCLUSIONS AND OUTLOOK

In this work, modal, harmonic, as well as linear and nonlinear transient FEM numeric analyses of the behaviour of the conventional three-layer design of piezoelectric vibration energy scavengers are performed. Mechanical dynamic response, the influence of mesh type and density as well as effects related to the electromechanical coupling are thus assessed. It is thus established that the eigenfrequencies resulting from FEM analyses are in excellent agreement with those obtained via the recently developed and experimentally verified coupled modal electromechanical distributed parameter model. The maximal voltage outputs and eigenfrequencies obtained from the FEM harmonic analyses match well analytical results as well, and coarser meshes based on brick elements seem already suitable to achieve this correspondence. The hardening effect induced by the backward piezoelectric coupling, causing a rise in eigenfrequencies for increasing electrical loads, is also clearly visible in the FEM results. However, the numerically obtained maximal voltage levels seem to be accurate only for electrical loads limited to roughly 100 kΩ (which should in any case satisfy the vast majority of practical applications), while for larger loads the discrepancies with respect to analytical and experimental data become significant and are probably due to the limitations of the used ANSYS® FEM modelling software already evidenced in literature. On the other hand, transient FEM analyses allowed establishing that an excellent matching with the implemented analytical model is achievable, albeit through a time-consuming, computationally intensive and cumbersome procedure. The nonlinear effects seem, however, to have a limited influence on the overall behaviour of the considered class of energy scavenging devices.

A cantilever characterised by an intricate multilayer structure, based on commercially available energy scavengers, not investigated so far in literature, is considered next. A corresponding experimental set-up is put in place to assess the validity of the developed FEM model. Different scavenger geometries with diverse tip mass and electric resistance loading conditions are considered in this frame both numerically and experimentally. A satisfying agreement between the numerical and the experimental results is achieved in terms of the dynamics behaviour of the considered devices in the presence of electromechanical coupling. In fact, FEM analyses' results predict again effectively the eigenfrequencies as well as the hardening effect due to backward coupling, confirming, however, once more the limit in the accurate prediction of the attained voltage levels to electrical loads limited to roughly (practically relevant) few tens of kΩ.

In future work the authors plan to use the developed FEM routines to model the behaviour of piezoelectric vibration scavengers in the 'plucking' (repetitive impact at the free end of cantilever) excitation mode to be used for effectively powering wireless sensor nodes for pollution monitoring in watercourses (cf. [35]). The authors will also explore the possibility of using the FEM approach to optimise the performances of piezoelectric vibration energy scavenging devices in terms of the attainable output powers per (minimised) device volume by improving their geometries and frequency bandwidths while taking into consideration the respective strength constraints.

ACKNOWLEDGEMENTS

This work is supported by the EU FP7 ICT-2009.9.1 project no. 269985 "GOLDFISH – Detection of Watercourse Contamination in Developing countries using Sensor Networks – Enlarged".

The authors acknowledge the kind help of the colleagues of the Laboratory of Mechanics of the Department of Electric, Managerial and Mechanic Engineering of the University of Udine, Italy.

REFERENCES

[1] Erturk, A. and Inman, D., [Piezoelectric energy harvesting], John Wiley & Sons, Chichester (2011).
[2] Kazmierski, T. and Beeby, S. (ed.), [Energy Harvesting Systems: Principles, Modeling and Applications], Springer (2011).
[3] Priya, S. and Inman, D. (ed.), [Energy Harvesting Technologies], Springer, New York (2009).
[4] Roundy, S., [Energy Scavenging for Wireless Sensor Nodes with a Focus on Vibration to Electricity Conversion], Ph. D. thesis, U. California, Berkeley (2003).
[5] Beeby, S. P., Tudor M. J. and White, N. M., "Energy harvesting vibration sources for microsystems applications," Meas. Sci. Technol. 17, 175-195 (2006).
[6] Mateu, L. and Moll, F., "Review of Energy Harvesting Techniques and Applications for Microelectronics," Proc. SPIE 5837 – VLSI Circuits and Systems II, 359-373 (2005).
[7] Torah, R., Glynne-Jones, P., Tudor, M. J., O'Donnell, T., Roy, S. and Beeby, S. P., "Self-powered autonomous wireless sensor node using vibration energy harvesting," Meas. Sci. Technol. 19, 125202 (2008).
[8] Erturk, A., [Electromechanical modeling of piezoelectric energy harvesters], Ph. D. thesis, Virginia Polytech. Inst. & State U. (2009).
[9] Benasciutti, D., Moro, L., Zelenika, S., and Brusa, E., "Vibration energy scavenging via piezoelectric bimorphs of optimized shapes," Microsys. Technol. 16/5, 657-668 (2010).
[10] Elvin, E. and Elvin, A., "A coupled finite element – circuit simulation model for analyzing piezoelectric energy generators," J. Intel. Mat. & Sys. Struct. 20, 587-595 (2009).
[11] Yang, Y. and Tang, L., "Equivalent circuit modeling of piezoelectric energy harvesters", J. Intel. Mat. & Sys. Struct. 20, 2223 (2009).
[12] Zhu, D., Almusallam, A., Beeby, S. P., Tudor, M. J. and Harris, N., "A bimorph multi-layer piezoelectric vibration energy harvester," PowerMEMS, Leuven, Belgium (2010).

[13] Zhu, M. et al., “Analysis of power output of piezoelectric energy harvesting devices directly connected to a resistive load using a coupled piezoelectric-circuit finite element method,” IEEE Trans. Ultras., Ferroel. & Freq. Contr. 56/7, 1309-1317 (2009).
[14] Ansys Inc., [Ansys Help] (2010).
[15] Ansys Inc., [Ansys Theory] (1994).
[16] Zelenika, S. and Blažević, D., “Issues in validation of performances of piezoelectric vibration-based energy harvesters,” Proc. SPIE 8066 – Smart Sens., Act. & MEMS V, 806615 (2011).
[17] Erturk, A. and Inman, D., “An experimentally validated bimorph cantilever model for piezoelectric energy harvesting from base excitation”, Smart Mat. & Struct. 18, 025009 (2009).
[18] CTS Electronic Components Inc., [PZT5A & 5H Materials Technical Data].
[19] Nash, D., “Transient Analysis,” - lecture, U. Strathclyde, Glasgow, UK.
[20] Meirowitch, L., [Fundamentals of Vibrations], McGraw Hill, Boston (2001).
[21] De Bona, F. and Zelenika, S., “A generalized Elastica-type approach to the analysis of large displacements of spring-strips,” J. Mech. Eng. Sci. – Proc. Inst. Mech. Eng. C 211/7, 509-517 (1997).
[22] Ashwell, D. G., “The anticlastic curvature of rectangular beams and plates,” J. Royal Aer. Soc., 708-715 (1950).
[23] De Bona, F., Zelenika, S. and Munteanu, M. Gh., “Mechanical properties of microcantilevers: Influence of the anticlastic effect,” Sens. Act. A 165/2, 431-438 (2011).
[24] Midé Technology Corporation, [Volture Products Spec Sheet & Material Properties] & [Volture Piezoelectric Energy Harvesters] (2009).
[25] ‹http://www.mide.com/› (10 June 2014). www.mide.com/
[26] Nippon Steel Chemical Co. Ltd., [ESPANEX SPC Series catalogue].
[27] Ražnjević, K. (ed.), [Krautov strojarski priručnik], Axiom, Zagreb (1997).
[28] ‹http://english.civa.no/home.aspx?docid=153› (10 June 2014). english.civa.no/home.aspx?docid=153
[29] ‹http://www.mbdynamics.com/PDF/PM-SERIES.pdf› (13 July 2014). www.mbdynamics.com/PDF/PM-SERIES.pdf
[30] ‹http://www.bksv.com/products/transducers/vibration/accelerometers/accelerometers/4375› (13 July 2014). www.bksv.com/products/transducers/vibration/accelerometers/accelerometers/4375
[31] ‹http://www.micro-epsilon.com/download/manuals/man--optoNCDT-1607--en.pdf› (13 July 2014). www.micro-epsilon.com/download/manuals/man--optoNCDT-1607--en.pdf
[32] ‹http://www.bksv.com/products/transducers/conditioning/charge/2635› (13 July 2014). www.bksv.com/products/transducers/conditioning/charge/2635
[33] ‹http://www.testequipmentconnection.com/specs/Bruel_Kjaer_1047.pdf› (13 July 2014). www.testequipmentconnection.com/specs/Bruel_Kjaer_1047.pdf
[34] ‹http://sine.ni.com/nips/cds/view/p/lang/hr/nid/13909› (13 July 2014). sine.ni.com/nips/cds/view/p/lang/hr/nid/13909
[35] Kamenar, E., Maćešić, S., Gregov, G., Blažević, D., Zelenika, S., Marković, K. and Glažar V., “Autonomous solutions for powering wireless sensor nodes in rivers,” these proceedings.